Volume 55 | Number 90 | 21 November 2019 | Pages 13475–13616

ChemComm

Chemical Communications

rsc.li/chemcomm

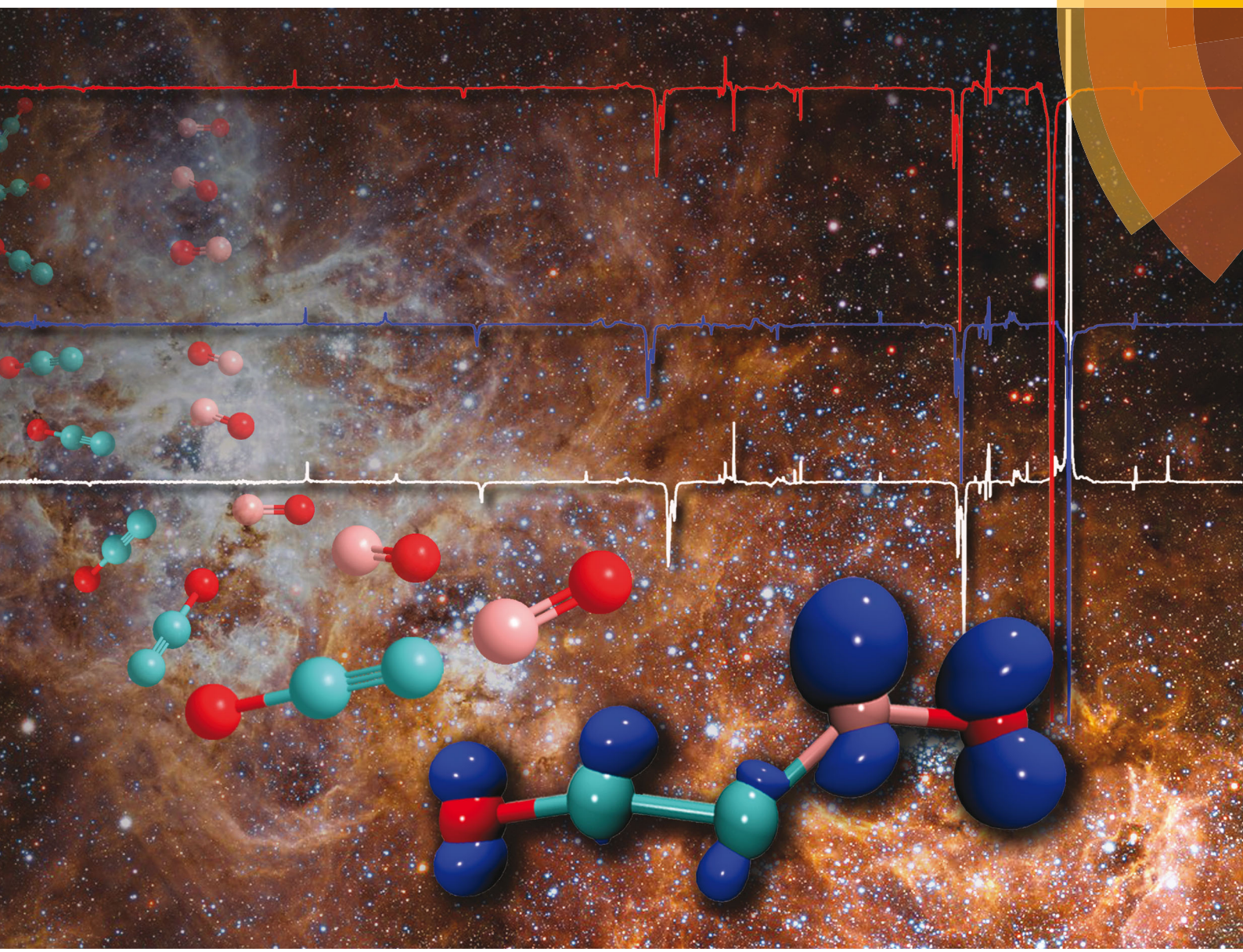

ISSN 1359-7345

ROYAL SOCIETY OF CHEMISTRY | Celebrating IYPT 2019

COMMUNICATION

Xiaoqing Zeng *et al.*

Heterocumulenic carbene nitric oxide radical OCCNO•

ChemComm

COMMUNICATION

Heterocumulenic carbene nitric oxide radical OCCNO•†

Bo Lu,[a] Chao Song,[a] Weiyu Qian,[a] Zhuang Wu,[a] Attila G. Császár[b] and Xiaoqing Zeng *[ac]

Cite this: *Chem. Commun.*, 2019, **55**, 13510

Received 10th September 2019,
Accepted 25th September 2019

DOI: 10.1039/c9cc07056g

rsc.li/chemcomm

The elusive heterocumulenic radical OCCNO• and its isotopologues $OC^{13}CNO^{\bullet}$ and $OCC^{15}NO^{\bullet}$ have been prepared by reacting photolytically generated unsaturated carbene OCC/$OC^{13}C$ with •NO/^{15}•NO in cryogenic N_2-, Ar-, and Ne-matrices. Upon UV-light (365 nm) irradiation, the C–C bond in OCCNO• breaks and yields a long-sought ground-state radical CNO• ($X^2\Pi$), which has also been identified with matrix-isolation infrared spectroscopy.

Carbon suboxide (OCCCO) is a five-atomic heterocumulene that contains 24 valence electrons. Its original synthesis dates back to the 1900s[1] and the structural and bonding properties of OCCCO and its isoelectronic analogues, such as neutral OCB(H)CO,[2] anionic $OCBCO^-$,[3] and cationic $OCNCO^+$,[4] still attract attention. OCCCO is a bent molecule in the gas phase ($\angle$(CCC) = 156°),[5] but it is linear in the solid state due to rather low barrier to linearity (<0.5 kcal mol^{-1}).[5,6] According to the latest bonding analyses,[2a,7] OCCCO can be best described as a Lewis adduct (OC → C ← CO) rather than a conventional cumulenic O=C=C=C=O molecule (**1**, Scheme 1). A similar dative-bond structure has been proposed for the nitrogen analogue $OCNCO^+$,[2] which has been structurally characterized in $[OCNCO]^+[Sb_3F_{16}]^-$ ($\angle$(CNC) = 130.7°),[4a] and for the highly energetic pentanitrogen cation $NNNNN^+$.[2,8]

In contrast to the cation, the neutral molecule OCNCO• (**2**), an analogue of the experimentally detected OCBCO,[3,9] ONNCO,[10] and $NCNO_2$[11] species, eluded observation. Attempts to generate **2** by neutralization of $OCNCO^+$ in the gas phase failed, and only fragments were detected by means of neutralization–reionization mass spectrometry (NRMS). The existence of the OCCNO• (**3**) isomer was inferred from the recovery signal for $OCCNO^+$ in NRMS experiments.[12] OCCNO• has been proposed as the key intermediate in the reaction of ketenylidene (C_2O) and •NO,[13] an elementary step in the formation and removal of NO_x during the combustion of unsaturated hydrocarbons.[14–17]

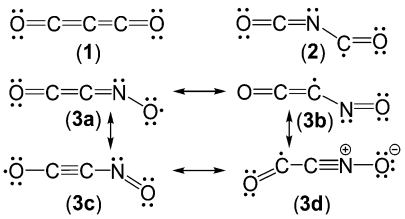

Scheme 1 Representations of the structures of OCCCO (**1**), OCNCO• (**2**), and OCCNO• (**3a–3d**).

According to the previous *ab initio* electronic-structure computations at the QCISD(T)/6-311G(2df,2pd) level, the C–C and C–N bond dissociation energies in OCCNO• are 9.7 (→ OC + •CNO) and 55.9 kcal mol^{-1} (→ C_2O + •NO), respectively.[13b] Therefore, OCCNO• should be a viable species for spectroscopic detection at low temperatures, and its decomposition through cleavage of the C–C bond might provide access to the CNO• radical, for which no experimental data exist for the electronic ground state ($X^2\Pi$),[19] and only the IR frequencies of the excited state ($A^2\Sigma^+$, 2239 and 1247 cm^{-1}) have been obtained in the Ne matrix.[18]

As an unsaturated carbene, C_2O forms complexes with transition metals such as Ru,[20] Fe,[21] and Au.[22] Recently, the reactions between N-heterocyclic carbenes (NHCs) and •NO were studied in solution at −78 °C, and metastable NHC-stabilized nitric oxide radicals were isolated.[23] According to the electronic-structure computations at the B3PW91/6-31G(d,p) level, the activation barrier for the association of •NO with NHCs is about 8.6 kcal mol^{-1}. Herein, we report the formation of OCCNO• by reacting •NO and C_2O in cryogenic matrices. The IR spectroscopic identification of OCCNO• and its decomposition product CNO• is supported by isotope labeling (^{13}C and ^{15}N) and advanced *ab initio* quantum-chemical computations.

[a] *College of Chemistry, Chemical Engineering and Materials Science, Soochow University, 215123 Suzhou, China. E-mail: xqzeng@suda.edu.cn*
[b] *MTA-ELTE Complex Chemical Systems Research Group, Laboratory of Molecular Structure and Dynamics, Institute of Chemistry, ELTE Eötvös Loránd University, Pázmány Péter sétány 1/A, H-1117 Budapest, Hungary*
[c] *Department of Chemistry, Fudan University, 200433 Shanghai, China. E-mail: xqzeng@fudan.edu.cn*

† Electronic supplementary information (ESI) available. See DOI: 10.1039/c9cc07056g

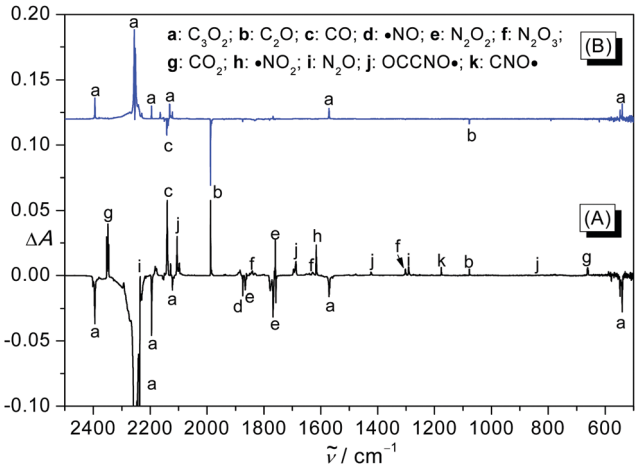

Fig. 1 (A) IR difference spectrum reflecting the changes of a mixture of OCCCO/•NO/N_2 = 1 : 5: 1000 upon 266 nm laser irradiation (65 min) at 15 K. (B) IR difference spectrum reflecting the changes of the mixture upon subsequent 830 nm LED irradiation (1 min).

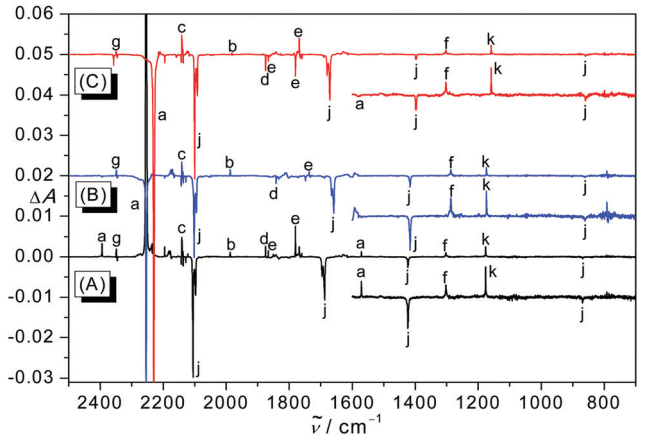

Fig. 2 (A) IR difference spectrum reflecting the depletion of OCCNO• in the N_2 matrix upon 365 nm LED irradiation (2.5 min) at 15 K. (B) IR difference spectrum reflecting the depletion of OCC^{15}NO• in the N_2 matrix upon 365 nm LED irradiation (2 min) at 15 K. (C) IR difference spectrum reflecting the depletion of OC^{13}CNO• in the N_2 matrix upon 365 nm LED irradiation (2 min) at 15 K. For clarity, each spectrum in the range of 1600–700 cm^{-1} is displayed after 3-times-expansion along the ΔA axis.

Consistent with the previous studies on CCO,[24] this species with a triplet ground electronic state ($X^3\Sigma$) can be generated during the UV photolysis (266 nm) of OCCCO (Fig. S1, ESI†). When the photolysis is performed in the presence of excessive •NO (OCCCO/•NO = 1 : 5), the IR difference spectrum (Fig. 1A) obtained after the photolysis shows the depletion of OCCCO (a) and the formation of C_2O (b, 1987.5 and 1077.9 cm^{-1}),[24] CO (c, 2139.8 cm^{-1}),[25] N_2O_3 (f, 1840.9, 1629.7, and 1302.7 cm^{-1}),[26] CO_2 (g, 2348.5 and 661.8 cm^{-1}),[27] •NO_2 (h, 1615.9 cm^{-1}),[28] N_2O (i, 2235.5 and 1291.2 cm^{-1}),[29] and a new species (j), with IR bands at 2106.9, 1688.3, 1423.3, and 868.7 cm^{-1}.

To distinguish the IR bands, the matrix was further irradiated with an 830-nm LED. The corresponding IR difference spectrum (Fig. 1B) demonstrates the depletion of C_2O and CO with the sole reformation of OCCCO, whereas the IR bands for •NO (1874.3 cm^{-1}) and the new species (j) remain unchanged. The preference for C_2O to combine with CO instead for •NO implies that most CO molecules can hardly escape from the solid N_2 matrix cages at 15 K, and the formation of OCCCO is probably more favorable than the formation of OCCNO•. The recombination of CCO with CO resembles the carbonylation of NHCs yielding ketenes.[30]

Following red-LED irradiation, the matrix was further photolyzed with an UV LED (365 nm), which selectively destroyed the carrier for the aforementioned four new IR bands (Fig. 2A). As a result, OCCCO (a), C_2O (b), CO (c), •NO (d), N_2O_2 (e), and N_2O_3 (f) were formed. To aid the assignment of the spectrum, isotope-labeling experiments using •^{15}NO (Fig. 2B) and OC^{13}CCO (Fig. 2C) as precursors have been performed. The corresponding IR difference spectra (Fig. S2, ESI†) after red-LED irradiation further verify the reformation of OCCCO. As expected, all the four IR bands, at 2106.9, 1688.3, 1423.3, and 868.7 cm^{-1}, most likely the signatures of OCCNO•, display noticeable isotopic shifts (Table 1).

The strongest band at 2106.9 cm^{-1} shifts only slightly, by 4.0 and 5.4 cm^{-1} in OCC^{15}NO• and OC^{13}CNO•, respectively, and it is assigned to the asymmetric CCO stretching vibration (ν_{asym}(CCO)) with a minor contribution from the asymmetric CNO stretch (ν_{asym}(CNO)). The observed wavenumber is supported by the value of ν_{calc} = 2148 cm^{-1} computed at the UCCSD(T)/cc-pVDZ level after correcting the harmonic value with the UBP86/6-311+G(3df) calculated anharmonic contribution (53 cm^{-1}, Table 1). The measured wavenumber is lower than the ν_{asym}(CCO) mode in ketenes, as in OCCCO (2254.7 cm^{-1}, Ar-matrix) and H_2CCO (2142 cm^{-1}, Ar-matrix),[31] but higher than those in the ketenyl radical HCCO• (2019.5 cm^{-1}, Ar-matrix),[32] gold ketenylidene Au_2CCO (2040 cm^{-1}, Au-surface),[22] and carbonyl cyanide radical (NCCO•, 1889.2 cm^{-1}, N_2-matrix).[33] The band at 1688.3 cm^{-1} belongs to ν_{asym}(CNO) (ν_{calc} = 1715 cm^{-1}), supported by large ^{15}N and ^{13}C isotope shifts of 29.9 and 16.4 cm^{-1}, respectively. This wavenumber is higher than ν(NO) in CF_3NO (1593.5 cm^{-1}, $\Delta\nu(^{15/14}N)$ = 26.9 cm^{-1} in an Ar-matrix)[34] but significantly lower than ν_{asym}(CNO) in acetonitrile *N*-oxide ($CH_3C{\equiv}N^+–O^-$, 2309 cm^{-1} in an Ar matrix).[35] In line with the calculated ^{15}N and ^{13}C isotope shifts of 6.9 and 25.5 cm^{-1}, respectively, for the symmetric CNO stretching mode (ν_{sym}(CNO)), the band at 1423.3 cm^{-1} (ν_{calc} = 1436 cm^{-1}) shifts by 6.9 and 25.0 cm^{-1}, respectively. The observed weakest band at 868.7 cm^{-1} (ν_{calc} = 881 cm^{-1}) corresponds to the symmetric stretch of the CCN moiety, and its assignment is also supported by the ^{15}N and ^{13}C isotopic shifts (Table 1).

The photosensitivity of OCCNO• upon 365 nm LED irradiation coincides with the calculated vertical transition at 324 nm with an oscillator strength (f) of 0.005, computed at the TD-BP86/6-311+G(3df) level. Among the IR bands for the photolysis (365 nm) products of OCCNO• (Fig. 2), one band at 1176.5 cm^{-1} (*k*) distinguishes itself from others by the occurrence of both ^{15}N and ^{13}C isotope shifts (2.5 and 17.7 cm^{-1}, respectively), indicating that both atoms are part of the carrier. Given the unimolecular decomposition of OCCNO• in the solid N_2 matrix and the

Table 1 Calculated and observed IR data of OCCNO•

Calculated				Observed			Isotope shifts				
UBP86/6-311+G(3df)[a]		UCCSD(T)/cc-pVDZ		Matrix[d]			$\Delta\nu$ (OCC$^{14/15}$NO•)		$\Delta\nu$ (OC$^{13/12}$CNO•)		
ν_{harm}	ν_{anharm}	ν_{harm}[b]	ν_{anharm}[c]	N_2 matrix	Ne matrix	Ar-matrix	Calc[e]	Obs[f]	Calc[e]	Obs[f]	Observed[g]
2141 (944)	2088 (785)	2201 (1042)	2148	2106.9 (100)	2106.5 (100)	2098.6 (100)	0.1	4.0	9.0	5.4	ν_{asym}(CCO)
1750 (404)	1718 (389)	1747 (929)	1715	1688.3 (55)	1691.7 (57)	1693.8 (52)	31.8	29.9	17.3	16.4	ν_{asym}(CNO)
1445 (129)	1422 (112)	1459 (5)	1436	1423.3 (8)	1423.4 (4)	1427.0 (6)	6.9	6.9	25.5	25.0	ν_{sym}(CNO)
882 (10)	833 (9)	930 (66)	881	868.7 (1)	876.2 (1)	869.4 (1)	8.5	7.9	9.6	9.4	ν_{sym}(CCN)
563 (9)	557 (8)	611 (12)	605				1.5		1.9		$\delta_{o.o.p.}$(CCO)
501 (9)	492 (9)	576 (18)	567				4.2		1.6		$\delta_{i.p.}$(CCN)
462 (3)	444 (3)	513 (5)	493				3.7		0.8		$\delta_{i.p.}$(CCO)

[a] UBP86/6-311+G(3df) calculated harmonic and anharmonic IR frequencies (>400 cm^{-1}) and intensities (km mol^{-1}, in parentheses). [b] UCCSD(T)/cc-pVDZ calculated harmonic IR frequencies and intensities (km mol^{-1}, in parentheses). [c] Corrected with UBP86/6-311+G(3df) anharmonic contributions. [d] Observed positions in different matrices and the relative intensities (in parentheses). [e] Isotope shifts calculated at the UCCSD(T)/cc-pVDZ level. [f] Observed isotope shifts in the N_2 matrix. [g] Assignment based on the calculated vibrational displacement vectors at the UBP86/6-311+G(3df) level.

simultaneous formation of CO, it is very likely that this band belongs to the counterpart fragment, CNO•. To confirm this hypothesis, computations were performed on the IR spectrum of the CNO• radical in its electronic ground state ($X^2\Pi$). At the UBP86/6-311+G(3df) level the two harmonic stretching fundamentals are at 1844 and 1172 cm^{-1}. The former band is computed to be too weak to be observable. This is in line with the lack of experimental observation of this line. However, the latter band has a computed IR intensity of 61 km mol^{-1}, and the calculated ^{15}N and ^{13}C isotope shifts of 1.5 and 19.9 cm^{-1}, respectively, agree with the observations. The assignment is also supported by the good agreement of the observed band with the MRCI(Q)-F12/VQZ-F12 calculated harmonic wavenumber of 1185 cm^{-1}.[19a] The bending fundamental of CNO• (ν_{calc} = 349 cm^{-1}) lies outside the available spectral range (4000–500 cm^{-1}). The "symmetric" stretching fundamental of CNO• ($X^2\Pi$) occurs at 1171.2 and 1167.3 cm^{-1} in Ar and Ne matrices, respectively.

To estimate the thermal stability of OCCNO•, the potential energy profiles of two of its dissociation channels have been explored (Fig. S4–S6, ESI†). In sharp contrast to an activation barrier (22.6 kcal mol^{-1}, B3PW91/6-31G(d,p)) for the C–N bond cleavage in the metastable NHC-stabilized nitric oxide radicals,[22] the highly endothermic C–N bond cleavage in OCCNO• (→ OCC + NO•) needs to overcome a substantial barrier of about 63 kcal mol^{-1} (UB3LYP/6-311+G(3df)). According to our focal-point analysis (FPA)[36] study (Tables S1–S4, ESI†), the C–N bond dissociation energy (BDE) is as large as 62.2(22) kcal mol^{-1}. Consistent with the observed fragmentation into CO and CNO•, the FPA value of the BDE of the C–C bond cleavage in OCCNO• (→ OC + CNO•) is 15.7(20) kcal mol^{-1} and it needs to overcome a lower barrier of about 26 kcal mol^{-1} (UB3LYP/6-311+G(3df)).

OCCNO• is a strongly bent planar molecule in which the OCC and NO moieties adopt a *trans* configuration with respect to the C–N bond (Fig. 3A). There is no minimum in the region of the *cis* conformer. The OCC, CCN, and CNO angles in OCCNO• are 166.5°, 128.9°, and 137.5° at the frozen-core ROCCSD(T)/aug-cc-pVQZ level, implying contributions from all four mesomeric Lewis structures bearing free valence electrons at each atom (**3a–3d**, Scheme 1). The OCC angle in

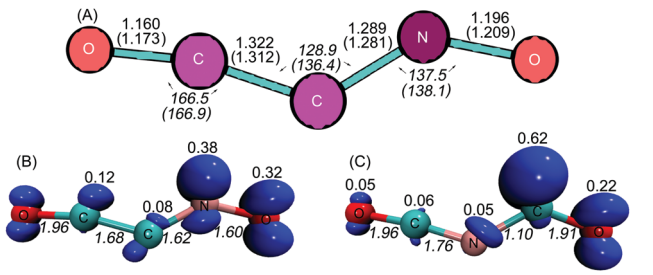

Fig. 3 (A) Calculated molecular structures for OCCNO• (bond lengths in Å, angles in degrees in italics) at the ROCCSD(T)/aug-cc-pVQZ and UBP86/6-311+G(3df) (in parentheses) levels. (B) Calculated spin densities and Wiberg bond indices (WBI) for OCCNO• (in italics) at the UBP86/6-311+G(3df) level. (C) Calculated spin densities and WBI for OCNCO• (in italics) at the UBP86/6-311+G(3df) level.

OCCNO• (166.5°) is significantly larger than that in OCCN• (132.2°, all-electron ROCCSD(T)/cc-pCVQZ);[33b] hence, OCC in OCCNO• is a weakened ketene moiety with an observed frequency of 2106.9 cm^{-1} (ν_{asym}(CCO), N_2 matrix). Note that OCCN• is a carbonyl radical with a typical C=O stretching fundamental (ν(CO)) at 1889.2 cm^{-1} (N_2 matrix).[33a] A considerably larger CCN angle (136.4°) was calculated for OCCNO• at the DFT (UBP86/6-311+G(3df)) level, and the other DFT structural parameters are quite similar to those obtained at the ROCCSD(T)/aug-cc-pVQZ level (Fig. 3A).

According to the natural bond order (NBO) analysis, the Wiberg bond index (WBI) for the terminal C=O moiety in OCCNO• is 1.96 (Fig. 3B). The other three bonds have nearly identical WBIs of about 1.6 due to delocalization. In line with the bonding characteristics, the spin densities for the unpaired electron mainly localized on the terminal NO moiety (N: 0.38; O: 0.32), and the CO moiety carries a total spin density of only 0.22. Therefore, OCCNO• can be regarded as a mixture of the resonance structures of an iminoxyl radical (**3a** in Scheme 1), a ketenyl radical (**3b**), an ethynyloxyl radical (**3c**), and an acyl radical (**3d**), in which the last two probably play a less important role. In contrast, the putative isomer OCNCO• (Fig. 3C) is a carbonyl radical, as indicated by the total spin density of 0.84 on

the C═O moiety (WBI = 1.91) and the presence of a C–N single bond (WBI = 1.10) in the molecule.

In summary, a heterocumulenic radical OCCNO• has been generated by reacting •NO with photolytically prepared C_2O in cryogenic matrices. In addition to the IR spectroscopic identification of OCCNO•, by ^{13}C and ^{15}N labeling, its photodecomposition by breaking the C–C bond has also been observed, enabling IR spectroscopic characterization of the ground electronic state of the CNO• radical.

This work was supported by the National Natural Science Foundation of China (21673147) and the Priority Academic Program Development of Jiangsu Higher Education Institutions (PAPD). We thank Prof. Guntram Rauhut for some CCSD(T) calculations, Prof. Mingfei Zhou for providing the ^{15}NO sample, and Prof. Peter R. Schreiner for helpful comments. The work of AGC was supported by an NKFIH grant (K119658) and the ELTE Excellence Program (1783-3/2018/FEKUTSTRAT) supported by the Hungarian Ministry of Human Capacities (EMMI).

Conflicts of interest

There are no conflicts to declare.

Notes and references

1 O. Diels and B. Wolf, *Ber. Dtsch. Chem. Ges.*, 1906, **39**, 689–697.
2 (*a*) M. A. Celik, R. Sure, S. Klein, R. Kinjo, G. Bertrand and G. Frenking, *Chem. – Eur. J.*, 2012, **18**, 5676–5692; (*b*) H. Braunschweig, R. D. Dewhurst, F. Hupp, M. Nutz, K. Radacki, C. W. Tate, A. Vargas and Q. Ye, *Nature*, 2015, **522**, 327–330; (*c*) S. Riedel, M. Straka and P. Pyykkö, *THEOCHEM*, 2008, **860**, 128–136.
3 Q. Zhang, W.-L. Li, C.-Q. Xu, M. Chen, M. F. Zhou, J. Li, D. M. Andrada and G. Frenking, *Angew. Chem., Int. Ed.*, 2015, **54**, 11078–11083, and references therein.
4 (*a*) I. Bernhardi, T. Drews and K. Seppelt, *Angew. Chem., Int. Ed.*, 1999, **38**, 2232–2233; (*b*) P. Pyykkö, *Phys. Chem. Chem. Phys.*, 2012, **14**, 14734–14742; (*c*) R. G. Cooks, H. Chen, M. N. Eberlin, X. Zheng and W. A. Tao, *Chem. Rev.*, 2006, **106**, 188–211; (*d*) P. Pyykkö and N. Runeberg, *J. Mol. Struct.*, 1991, **234**, 279–290.
5 P. Jensen and J. W. C. Johns, *J. Mol. Spectrosc.*, 1986, **118**, 248–266.
6 A. Ellern, T. Drews and K. Seppelt, *Z. Anorg. Allg. Chem.*, 2001, **627**, 73–76.
7 R. Tonner and G. Frenking, *Angew. Chem., Int. Ed.*, 2007, **46**, 8695–8698.
8 (*a*) K. O. Christe, W. W. Wilson, J. A. Sheehy and J. A. Boatz, *Angew. Chem., Int. Ed.*, 1999, **38**, 2004–2009; (*b*) A. Viji, W. W. Wilson, V. Vij, F. S. Tham, J. A. Sheehy and K. O. Christe, *J. Am. Chem. Soc.*, 2001, **123**, 6308–6313.
9 (*a*) M. F. Zhou, N. Tsumori, L. Andrews and Q. Xu, *J. Phys. Chem. A*, 2003, **107**, 2458–2463; (*b*) T. R. Burkholder and L. Andrews, *J. Phys. Chem.*, 1992, **96**, 10195–10201.
10 (*a*) X. Q. Zeng, M. F. Ge, Z. Sun and D. X. Wang, *Inorg. Chem.*, 2005, **44**, 9283–9287; (*b*) A. A. Korkin, J. Leszczynski and R. J. Barlett, *J. Phys. Chem.*, 1996, **100**, 19840–19846; (*c*) T. M. Klapötke and A. Schulz, *Inorg. Chem.*, 1996, **35**, 7897–7904.
11 M. Rahm, G. Bélanger-Chabot, R. Haiges and K. O. Christe, *Angew. Chem., Int. Ed.*, 2014, **53**, 6893–6897.
12 (*a*) D. Sülzle, P. E. O'Bannon and H. Schwarz, *Chem. Ber.*, 1992, **125**, 279–283; (*b*) M. C. Carvalho, V. F. Juliano, C. Kascheres and M. N. Eberlin, *J. Chem. Soc., Perkin Trans. 2*, 1997, 2347–2352.
13 (*a*) D. G. Williamson and K. D. Bayes, *J. Am. Chem. Soc.*, 1967, **89**, 3390–3396; (*b*) W. D. Thweatt, M. A. Erickson and J. F. Hershberger, *J. Phys. Chem. A*, 2004, **108**, 74–79; (*c*) V. M. Donnelly, W. M. Pitts and J. R. McDonald, *Chem. Phys.*, 1980, **49**, 289–293.
14 H. Choi, D. H. Mordaunt, R. T. Bise, T. R. Taylor and D. M. Neumark, *J. Chem. Phys.*, 1998, **108**, 4070–4078.
15 K. H. Becker and K. D. Bayes, *J. Chem. Phys.*, 1968, **48**, 653–661.
16 K. D. Bayes, *J. Chem. Phys.*, 1970, **52**, 1093–1097.
17 A. Fontijn and S. E. Johnson, *J. Chem. Phys.*, 1973, **59**, 6193–6200.
18 V. E. Bondybey, J. H. English, C. W. Mathews and R. J. Contolini, *Chem. Phys. Lett.*, 1981, **82**, 208–212.
19 (*a*) C. E. M. Gonçalves, B. R. L. Galvão, V. C. Mota, J. P. Braga and A. J. C. Varandas, *J. Phys. Chem. A*, 2018, **122**, 4198–4207; (*b*) C. Léonard and G. Chambaud, *Chem. Phys. Lett.*, 2008, **458**, 24–28; (*c*) R. Prasad, *J. Chem. Phys.*, 2004, **120**, 10089–10100; (*d*) M. V. Alves, C. E. M. Gonçalves, J. P. Braga, V. C. Mota, A. J. C. Varandas and B. R. L. Galvão, *J. Phys. Chem. A*, 2019, **123**, 7195–7200.
20 W. S. Sim and D. A. King, *J. Am. Chem. Soc.*, 1995, **117**, 10583–10584.
21 M. J. Sailor and D. F. Shriver, *J. Am. Chem. Soc.*, 1987, **109**, 5039–5041.
22 I. X. Green, W. Tang, M. Neurock and J. T. Yates, Jr., *J. Am. Chem. Soc.*, 2012, **134**, 13569–13572.
23 (*a*) J. Park, H. Song, Y. Kim, B. Eun, Y. Kim, D. Y. Bae, S. Park, Y. M. Rhee, W. J. Kim, K. Kim and E. Lee, *J. Am. Chem. Soc.*, 2015, **137**, 4642–4645; (*b*) Y. Kim and E. Lee, *Chem. – Eur. J.*, 2018, **24**, 19110–19121.
24 (*a*) R. L. DeKock and W. Weltner, Jr., *J. Am. Chem. Soc.*, 1971, **93**, 7106–7107; (*b*) M. E. Jacox, D. E. Milligan, N. G. Moll and W. E. Thompson, *J. Chem. Phys.*, 1965, **43**, 3734–3746.
25 Y. Ogawara, A. Bruneau and T. Kimura, *Anal. Chem.*, 1994, **66**, 4354–4358.
26 E. L. Varetti and G. C. Pimentel, *J. Chem. Phys.*, 1971, **55**, 3813–3821.
27 L. Wan, L. Wu, A.-W. Liu and S.-M. Hu, *J. Mol. Spectrosc.*, 2009, **257**, 217–219.
28 R. V. S. Louis and B. Crawford, *J. Chem. Phys.*, 1965, **42**, 857–864.
29 A. Łapiński, J. Spanget-Larsen, J. Waluk and J. G. Radziszewski, *J. Chem. Phys.*, 2001, **115**, 1757–1764.
30 (*a*) C. Goedecke, M. Leibold, U. Siemeling and G. Frenking, *J. Am. Chem. Soc.*, 2011, **133**, 3557–3569; (*b*) U. Siemeling, C. Färber, C. Bruhn, M. Leibold, D. Selent, W. Baumann, M. von Hopffgarten, C. Goedecke and G. Frenking, *Chem. Sci.*, 2010, **1**, 697–704.
31 R. Hochstrasser and J. Wirz, *Angew. Chem., Int. Ed. Engl.*, 1989, **28**, 181–183.
32 M. E. Jacox and W. B. Olson, *J. Chem. Phys.*, 1987, **86**, 3134–3142.
33 (*a*) P. R. Schreiner, H. P. Reisenauer, E. Mátyus, A. G. Császár, A. Siddiqi, A. C. Simmonett and W. D. Allen, *Phys. Chem. Chem. Phys.*, 2009, **11**, 10385–10390; (*b*) A. C. Simmonett, F. A. Evangelista, W. D. Allen and H. F. Schaefer III, *J. Chem. Phys.*, 2007, **127**, 014306.
34 X. Q. Zeng, H. Beckers, H. Willner, P. Neuhaus, D. Grote and W. Sander, *J. Phys. Chem. A*, 2015, **119**, 2281–2288.
35 Z. Mielke, M. Hawkins and L. Andrews, *J. Phys. Chem.*, 1989, **93**, 558–564.
36 A. G. Császár, W. D. Allen and H. F. Schaefer III, *J. Chem. Phys.*, 1998, **108**, 9751–9764.